Low-SAR Trabecular Bone Micro-MRI for use at Ultra-High Field

J. F. Magland[1], A. C. Wright[1], H. Saligheh-Rad[1], and F. W. Wehrli[1]
[1]Department of Radiology, University of Pennsylvania Medical Center, Philadelphia, PA, United States

Introduction: Both spin-echo and gradient-echo approaches have been employed for high-resolution structural imaging of trabecular bone [1, 2], and the derived structural parameters have been able to detect small changes in trabecular bone architecture due to disease or treatment [3]. The primary limiting factor for this application is the signal-to-noise ratio (SNR), which inherently restricts the achievable resolution and the necessary scan time. The highest in vivo resolution reported at 1.5 Tesla within a clinically feasible scan time (~15 minutes) is on the order of 140x140 μm^2 with a slice thickness of approximately 400 µm. At 3 Tesla, where SNR efficiency is higher (theoretically by a factor of two), isotropic 150 µm resolution has been reported [4]. However, these data were acquired toward the lower limit of the acceptable SNR and toward the maximum tolerable scan time. The introduction of ultra-high field (e.g. 7 Tesla) whole-body scanners has the potential to enable acquisition of structural trabecular bone images at isotropic resolution at significantly reduced scan time, or alternatively at substantially increased SNR. However, the increased power deposition at the higher field strength may prevent the use of the 3D FLASE [5] spin-echo pulse sequence, which includes two high flip-angle pulses per repetition (one for excitation and one for refocusing). Here we investigate the use of two alternative pulse sequences for imaging trabecular bone at 7 Tesla: Hybrid radial variable echo time (HR-VTE) [6], and fractional-echo variable echo time (FE-VTE) with Cartesian sampling. In each of these sequences, a variable echo time is used to minimize the TE near the center of k-space, which is key to reducing susceptibility-induced phase spreading at the bone/bone-marrow interface.

Methods: The two pulse sequences (HR-VTE and FE-VTE) were implemented at 3 and 7 Tesla on Siemens TIM Trio scanners (diagrams are given in Fig. 1). Apart from the k-space sampling scheme, the sequences are identical (i.e. same minimum TE, TR, RF pulse, etc.) In the case of HR-VTE, radial views are acquired in two dimensions, with a golden angle increment between views [7], and phase encoding along the third (Z) direction. For FE-VTE, phase encoding is applied in both Y and Z directions, and only slightly more than half of k-space is acquired in the readout (X) direction. Echo time was variable, and minimized throughout the sequence, with TE = 1 ms at the center of k-space and a maximum echo time of 2 ms for HR-VTE and 3 ms for FE-VTE (that maximum echo time was greater for the Cartesian sequence because in-plane resolution was higher than slice resolution). The following parameters were used: truncated 20° sinc pulse, TR = 20 ms, resolution = 137x137x410 μm^3, 48 slices, and readout bandwidth of 64 Hz/pixel. A custom 4-channel surface receive coil (Insight MRI, Worcestor, MA) was used, with identical (horseshoe) geometry at the two field strengths. The distal tibiae of two male volunteers (age 30-40) were scanned at both field strengths.

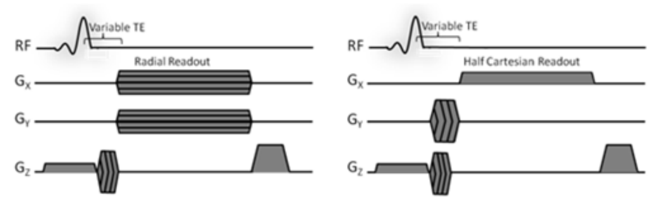

Fig. 1. Pulse sequence diagrams for (left) HR-VTE and (right) FE-VTE.

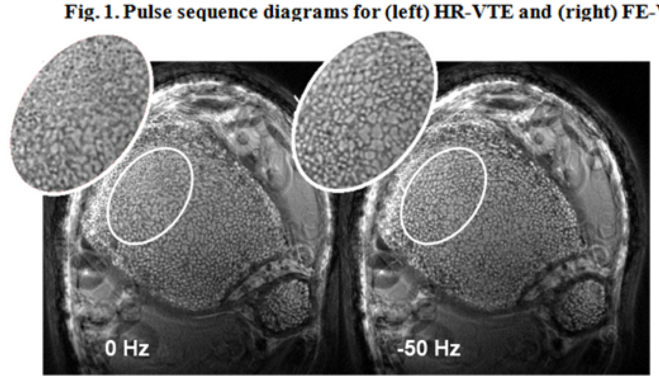

Fig.2. HR-VTE images of the distal tibia acquired at 7 Tesla and reconstructed at two different frequencies (0 Hz and -50 Hz offset from the scanner-calibrated value). Due to B_0 field inhomogeneity, different parts of the image need to be reconstructed with different frequency offsets.

Results and Discussion: There are mutual tradeoffs for the two sequences. The primary advantage of the radial sequence is that it offers the capability of motion correction, either via low-resolution subaperture images reconstructed throughout the scan [8], or by using a center-of-mass type technique for tracking translational motion [9]. The Cartesian sequence has no such options, and unlike FLASE, there is no time for separate navigator acquisitions throughout the sequence. The primary disadvantage of HR-VTE is its susceptibility to off-resonance effects. Fig. 2 shows HR-VTE images acquired at 7 Tesla and reconstructed using two different resonance frequency offsets. In the magnified region, the image on the right is clearly sharper, whereas, the image on the left is sharper in the right-posterior portion of the bone. Therefore, the presence of B_0 field inhomogenity may require separate reconstructions for different regions of the image. The Cartesian sequence has no such problem, and has a further advantage that reconstruction time is considerably shorter.

Both sequences were able to depict the trabecular bone structure at high resolution, without significant artifacts. However, image quality seemed to be significantly better with the radial sequence. We attribute this observation to the fact that the echo time varies only in the slice encode (Z) direction for HR-VTE, whereas TE is variable along both Y and Z encoding directions for FE-VTE.

Conclusions: The feasibility of high-resolution trabecular bone imaging of the distal tibia at high and ultra-high field has been demonstrated using a pair of relatively low-SAR variable echo time sequences. The hybrid radial sequence appears to give the best image quality, although reconstruction time and off-resonance effects are challenges to be addressed. Future work will focus on optimizing the pulse sequence and reconstruction algorithms, and using the SNR gain afforded by increased field strength to achieve isotropic resolution with reduced scan time relative to that achievable at lower field.

References: [1] Wehrli et al, Proc IEEE 91:1520-1542 (2003); [2] Majumdar et al, Top Magn Reson Imaging 13:323-334 (2002) [3] Wehrli et al, J Bone Miner Res 23:730-740 (2008); [4] Magland et al, 16th ISMRM, Toronto (2008); [5] Ma et al, Magn Reson Med 35:903-910 (1996); [6] Magland et al, 13th ISMRM, Miami (2005); [7] Winkelmann et al, IEEE Trans Med Imaging 26:68-76 (2007); [8] Song et al, Magn Reson Med 46:503-509 (2001); [9] Welch et al, Magn Reson Med 52:337-45 (2004). **Acknowledgement:** NIH grant R01 AR 53156